

## X-ray resonant scattering in the ferromagnet CoPt

F. de Bergevin

*European Synchrotron Radiation Facility, Boîte Postale 220, F-38043 Grenoble CEDEX, France  
and Laboratoire de Cristallographie, Centre National de la Recherche Scientifique, 166X F-38042 Grenoble CEDEX, France*

M. Brunel

*Laboratoire de Cristallographie, Centre National de la Recherche Scientifique, 166X F-38042 Grenoble CEDEX, France*

R. M. Galéra

*Laboratoire de Magnétisme Louis Néel, Centre National de la Recherche Scientifique,  
166X F-38042 Grenoble CEDEX, France*

C. Vettier

*European Synchrotron Radiation Facility, Boîte Postale 220, F-38043 Grenoble CEDEX, France*

E. Elkäim, M. Bessière, and S. Lefèbvre

*Laboratoire pour l'Utilisation du Rayonnement Electromagnétique, Université de Paris-Sud, F-91405 Orsay CEDEX, France*

(Received 26 December 1991; revised manuscript received 10 July 1992)

Resonant enhancement of the magnetic x-ray scattering has been observed in the ferromagnetic compound CoPt. By measuring the scattered Bragg intensities upon reversal of the magnetization perpendicular to the scattering plane, the asymmetry ratio has been determined for the (220), (331), and the (440) reflections. The resonant line shape of the asymmetry ratios was investigated by tuning the photon energy through the  $L_{III}$  edge of platinum. Values, as large as  $-0.012$ ,  $-0.07$ , and  $0.09$  for the (220), (331), and (440) reflections, respectively, are observed at the maximum of the resonance. These values are in agreement with the theoretical predictions made for a similar alloy  $Pt_3Mn$ . The resonant line shape of asymmetry ratios is accounted for by a single  $2p \leftrightarrow 5d$  dipolar electric transition and a magnetic scattering amplitude equal to  $0.8 r_0$  per platinum atom.

### INTRODUCTION

In the last several years a growing number of experiments on very different magnetic systems has been undertaken that use x-ray scattering. Owing to the high fluxes, polarization and tunability of synchrotron radiation, scattering of x-rays is becoming an experimental technique to investigate magnetic materials. Strong enhancements of the magnetic scattering have recently been observed in holmium<sup>1</sup> and UAs,<sup>2</sup> by tuning the energy of the incident photons through the  $L_{II}$ ,  $L_{III}$  or  $M_{IV}$ ,  $M_V$  absorption edges. This effect, also called resonant exchange scattering,<sup>3</sup> was observed in diffraction experiments on collinear antiferromagnetic or helimagnetic compounds, where purely magnetic superlattice peaks exist.<sup>1,2</sup> At the same time, studies in ferromagnetic systems<sup>4-8</sup> by absorption spectroscopy near the  $L$  or  $M$  edges with circularly polarized synchrotron radiation show important effects of magnetic dichroism. The enhancement of the magnetic signal, measured in both types of experiments, arises from the same mechanism. It has been analyzed by Hannon *et al.*<sup>3</sup> on the basis of electric multipole transitions between an atomic core level and either an unfilled atomic shell or a narrow band. To get a strong resonant enhancement, the scattering must involve a low-order electric multipole transition. The resonant exchange scattering is also increased when the spin-orbit coupling

splits the inner shell in a well-resolved doublet, as  $L_{II}$ - $L_{III}$  or  $M_{IV}$ - $M_V$ . Due to the Pauli exclusion principle, the transitions are allowed only to unoccupied states, which results in an *exchange interaction* sensitive to the magnetization of the  $f$  and  $d$  states.

Resonant exchange scattering can also be observed by diffraction experiments in ferro- or ferrimagnetic systems. An experiment was made by Namikawa *et al.*<sup>9</sup> at the  $K$  edge of Ni. While it showed a very small effect, Carra, Altarelli, and de Bergevin<sup>10</sup> predicted larger effects at the  $L$  edges of the  $5d$  transition metal or of the rare-earth systems where the inner shell is split into well-resolved  $L_{II}$  and  $L_{III}$  levels by a strong spin-orbit coupling. In a ferro- or ferrimagnet, the diffracted Bragg intensity contains a product of a magnetization-dependent and a non-magnetic amplitude. The intensity of the Bragg peaks can be changed by reversing the magnetization along a direction perpendicular to the diffraction plane and an asymmetry ratio  $R_a$  can be then defined. A large asymmetry ratio has indeed been observed by Kao *et al.*<sup>11</sup> at the  $L_{II}$  and  $L_{III}$  edges of iron. Since Bragg scattering is impossible at that energy, instead the reflectivity of a thin film was measured. The proposal by Carra *et al.* is to measure the asymmetry ratio of the Bragg peaks near the  $L_{II}$ - $L_{III}$  edges of the  $5d$  transition metal in  $3d$ - $5d$  intermetallics. For instance, in  $MnPt_3$ , where the Pt ions carry very weak magnetic moments of the order of only

$0.26\mu_B$ , asymmetry ratios as large as a few percent are predicted. We present in this paper a synchrotron radiation diffraction experiment on a quite similar ferromagnetic compound, CoPt. The evolution of the asymmetry ratio determined for the (220), (331), and (440) Bragg reflections has been observed near the  $L_{III}$  absorption edge of platinum.

The total coherent scattering amplitude in magnetic materials results from different contributions: the usual Thomson scattering,  $f_0$ , and the magnetic scattering. Magnetic scattering arises from interaction between the electromagnetic wave and both spin and orbital magnetization densities. This last contribution is smaller by  $(\hbar\omega/mc^2)$  in amplitude than the charge terms and will be neglected in the following discussion. The amplitude of the scattering can be expressed as a  $2 \times 2$  matrix defined in the basis of two polarization states of the photons, respectively perpendicular ( $\sigma$ ) and parallel ( $\pi$ ) to the scattering plane.

The scattering amplitude, choosing the unit as  $r_0$ , the electron radius, is given by

$$f = -(\hat{\mathbf{e}}_f^* \cdot \hat{\mathbf{e}}_i)(f_0 + f' - if'') + a_{\text{res}}. \quad (1)$$

$f', if''$  are the contributions from dispersive and absorptive processes. In Eq. (1) the convention for the sign of the imaginaries is that used in neutron diffraction. Equation (1) is written so as to represent the Thomson amplitude by a positive  $f_0$ . Subsequently,  $f'$  is negative and  $f''$  positive. These quantities describe the usual resonant charge scattering and are assumed to be magnetization independent. Scattering from specific electric multipole transitions between a core level and either an unfilled atomic shell or a narrow band has been put apart in  $a_{\text{res}}$ . It contains the magnetization-dependent resonant exchange scattering. In the present case, we will consider electric dipolar transitions in the absence of crystal field effects. Indeed, at the  $L_{III}$  edge of Pt only dipolar transitions  $2p_{3/2} \leftrightarrow 5d_{5/2}$  are expected. The resonant exchange scattering amplitude in units of  $r_0$  is written as<sup>3</sup>

$$a_{\text{res}} = \frac{i+x}{1+x^2} \{ \hat{\mathbf{e}}_f^* \cdot \hat{\mathbf{e}}_i (F_{11} + F_{1-1}) - i(\hat{\mathbf{e}}_f^* \times \hat{\mathbf{e}}_i) \cdot \hat{\mathbf{z}} (F_{11} - F_{1-1}) + (\hat{\mathbf{e}}_f^* \cdot \hat{\mathbf{z}})(\hat{\mathbf{e}}_i \cdot \hat{\mathbf{z}})(2F_{10} - F_{11} + F_{1-1}) \}. \quad (2)$$

In Eqs. (1) and (2), the unit vector  $\hat{\mathbf{e}}_i$  ( $\hat{\mathbf{e}}_f$ ) represents the incident (scattered) polarization of the beam and  $\hat{\mathbf{z}}$  the direction of the quantization axis defined by the local moment of the ion. The  $F_{lm}$  terms are proportional to the probability of a  $l$ -polar virtual transition associated with a transfer  $m$  of angular momentum along the direction  $\hat{\mathbf{z}}$  of the quantization axis ( $m = 0 \pm 1$  for dipolar transitions). Their magnitude depends on overlap integrals between the atomic ground state and the intermediate excited one. In order to simplify the formulation, we use a notation for the  $F_{lm}$  slightly different from Refs. 3 and 10. In Eq. (2) the  $F_{lm}$  terms include all the constant factors. The energy-dependent factors are written as a function of  $x$ , the relative deviation from the resonance:

$$x = \frac{(E_f - E_i) - \hbar\omega}{\Gamma/2}. \quad (3)$$

$E_f - E_i$  is the transition energy and  $\hbar\omega$  the energy of the incident photons.

In a ferro- or ferrimagnetic system, the magnetization-dependent amplitude is mixed up in the same peak with Thomson and conventional dispersive amplitudes. It gives rise to an interference term which contains the factor

$$(\hat{\mathbf{e}}_f^* \cdot \hat{\mathbf{e}}_i)(\hat{\mathbf{e}}_f^* \times \hat{\mathbf{e}}_i) \cdot \hat{\mathbf{z}}. \quad (4)$$

Its sign changes on a magnetization reversal. Therefore it is possible to observe an asymmetry ratio  $R_a$  defined by

$$R_a = \frac{I^\uparrow - I^\downarrow}{I^\uparrow + I^\downarrow}. \quad (5)$$

$I^\uparrow$  ( $I^\downarrow$ ) represents the scattered intensity for spin parallel (antiparallel) to  $\hat{\mathbf{z}}$ . The factor (4) reaches its maximum value for a  $\pi$ - $\pi$  experimental scattering geometry and  $\hat{\mathbf{z}}$  parallel to  $\hat{\mathbf{k}}_i \times \hat{\mathbf{k}}_f$ . Such a configuration is easily obtained in a synchrotron experiment when the sample is kept single domain with the magnetization perpendicular to the horizontal diffraction plan. In these experimental conditions, the contribution of  $a_{\text{res}}$  to the total amplitude may be separated out in two terms. In Eq. (2), the first term, independent of the magnetization, accounts for the white line at the absorption edge. It can be expressed in a simplified formulation as  $F_{11} + F_{1-1} = n_p$ . The second term gives the purely magnetic contribution and may also be simplified as  $F_{11} - F_{1-1} = n_m$ . For a completely in-plane incident polarization, the third term cancels. It can be neglected for the polarization achieved in usual cases.

In order to describe in a crude model the dispersive amplitudes near the absorption edge we represent the density of states by a step function and convolute it by the factor describing the resonance

$$\frac{i+x}{1+x^2}.$$

It is assumed that the absorption edge and the white line are centered at the same energy and have the same width  $\Gamma$ . While for the imaginary part the convolution is straightforward and results in an arctangent, the real part gives rise to an integral which diverges at high energy. This is a nonphysical feature, coming from our model having a constant amplitude, while the real amplitude decreases roughly as  $E^{-3}$ . Being interested only in the region near the edge, we replace the divergent part by an arbitrary constant, and obtain

$$f' - if'' = n_c + \frac{n_s}{2} \ln(1+x^2) - i \left[ n_{cs} + \frac{n_s}{\pi} \left[ \arctan(-x) + \frac{\pi}{2} \right] \right], \quad (6)$$

where  $n_c$  (the arbitrary constant) represents the value of  $f'$  at its minimum of amplitude,  $n_s$  the amplitude step of  $f''$  at the edge, and  $n_{cs}$  its value below the edge. This allows us to give an expression of the asymmetry ratio:

$$R_a = \frac{2n_m \tan(2\theta_B) A}{n_m^2 \tan^2(2\theta_B) + (A^2 + B^2) \left[ 1 + \frac{1 - P_{\parallel}}{P_{\parallel} \cos^2(2\theta_B)} \right]} \quad (7)$$

with

$$A = f_0 + n_c + \frac{n_s}{2} \ln(1 + x^2) + x n_{cs} + x \frac{n_s}{\pi} \left[ \arctan(-x) + \frac{\pi}{2} \right],$$

$$B = x f_0 + x n_c + x \frac{n_s}{2} \ln(1 + x^2) - n_{cs} - \frac{n_s}{\pi} \left[ \arctan(-x) + \frac{\pi}{2} \right] - n_p.$$

Equation (7) takes into account the degree of linear incident polarization. The incident polarization is described with its two components  $P_{\parallel}$  and  $P_{\perp}$  related to the corresponding Stokes parameter  $N_1$  through  $P_{\perp} - P_{\parallel} = N_1$  and  $P_{\perp} + P_{\parallel} = 1$ . The asymmetry ratio depends on the energy and on the diffraction angle  $\theta_B$ . The sign of  $\theta_B$  in (7) is defined as the sign of  $(\hat{\mathbf{k}}_i, \hat{\mathbf{k}}_f, \hat{\mathbf{z}})$ . We recall that in  $R_a$ ,  $I^1$  is measured for spin along  $\hat{\mathbf{z}}$ , i.e., magnetization opposite to  $\hat{\mathbf{z}}$ .  $R_a$  has the sign of  $n_m$  for scattering angles  $\theta_B < 45^\circ$ ; it vanishes at  $\theta_B = 45^\circ$  and changes its sign for  $\theta_B > 45^\circ$ .

### EXPERIMENT

The intermetallic alloy CoPt crystallizes at high temperature in a disordered face-centered-cubic structure. Below 1100 K it undergoes a phase transformation into an ordered face-centered-tetragonal structure. However, the disordered phase may be stabilized at room temperature by a fast cooling from 1300 K. Both ordered and disordered phases are ferromagnetic at room temperature ( $T_C \approx 700$  K or higher<sup>12-14</sup>). The present experiment is carried out on a single crystal of CoPt in the disordered phase (the order parameter is roughly 0.05). The magnetic moments are reported as  $\mu_{Co} = 1.65\mu_B$  and  $\mu_{Pt} = 0.25\mu_B$  in the ordered phase.<sup>15</sup> The same values have been found for ordered CoPt<sub>3</sub>, which shows, when disordered, a decrease of  $\mu_{Co}$  down to  $1.3\mu_B$  and an increase of  $\mu_{Pt}$  up to  $0.45\mu_B$ .<sup>16</sup> The bulk magnetization measurements made on our sample at room temperature show that the saturation is reached at about 0.4 T for a magnetic applied field along an easy twofold axis (Fig. 1), and that the magnetization is  $2.08\mu_B$  per CoPt unit. Since some fraction of the cobalt, of order of 15%, is actually substituted with iron, we do not draw precise values for the moments and assume  $\mu_{Co} \approx 1.65\mu_B$  and  $0.25 < \mu_{Pt} < 0.45\mu_B$ . The sample is a disk, 1 mm thick and 10 mm diameter. It is cut along a 110 surface, which also contains the  $[1\bar{1}0]$  and  $[001]$  directions. The mosaic width is in the range  $0.5-1^\circ$ .

X-ray-diffraction experiments were performed at Laboratoire pour l'Utilisation du Rayonnement Electromagnétique on the D23 beam line.<sup>17</sup> A double

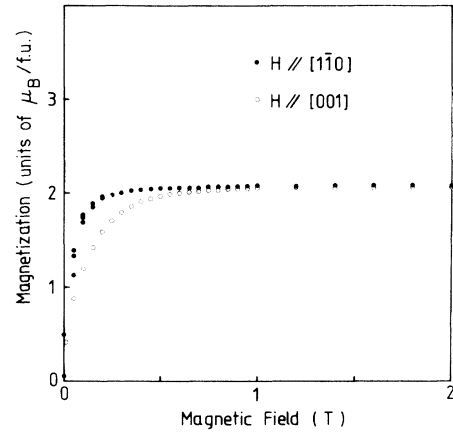


FIG. 1. Magnetization measurements at room temperature of the CoPt single crystal along the twofold  $[1\bar{1}0]$  (full dots) and the fourfold  $[001]$  (open dots) axes.

Si(311) monochromator allows one to tune the incident photon energy from 11 520 to 11 590 eV. The degree of linear polarization parallel to the horizontal scattering plane has been determined from the Bragg intensities of an aluminum powder. Five reflections, measured up to  $\theta_B = 40^\circ$ , give a good fit without any preferred orientation. The incident in-plane beam polarization  $P_{\parallel}$  was found to be 0.968. The experimental setup is drawn in Fig. 2. A small electromagnet, able to produce a magnetic field of 0.45 T, is mounted on the four circle diffractometer. The experimental geometry is set in order to have the axis of the  $\phi$  circle vertical and the magnetic field parallel to that axis ( $z$  in Fig. 2). The sample is mounted with its face parallel to the  $z$  axis on a fifth circle. This one is a small, manually driven, goniometer and allows one to align the  $[1\bar{1}0]$  or the  $[001]$  directions of the crystal parallel to the magnetic field, i.e., perpendicular to the horizontal scattering plane. We call it  $\psi$  circle, though its axis, normal to  $z$ , is along the scattering vector only for the  $(hh0)$  reflections. The evolution of the asym-

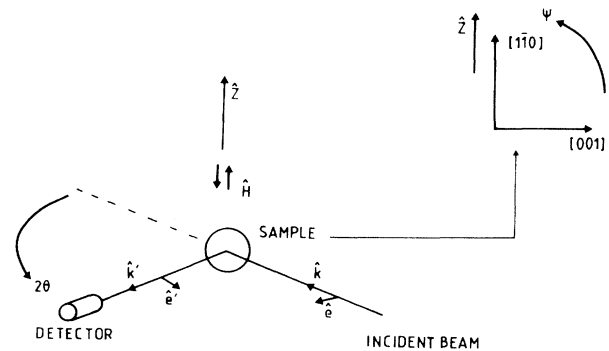


FIG. 2. Experimental setup. The diffraction plane is the horizontal plane and the applied magnetic field is perpendicular to it. The  $\psi$  movement represented in the inset allows one to align the sample with the  $[1\bar{1}0]$  or the  $[001]$  axis vertical, i.e., parallel to the field.

metry ratio as a function of the incident energy was determined by measuring the reflections (220), (331), and (440) at the Bragg angles  $23.7^\circ$ ,  $38.3^\circ$ , and  $53.6^\circ$ , respectively, with the  $[1\bar{1}0]$  direction of the crystal parallel to the magnetic field. For a given incident energy, the evolution of the asymmetry ratio as a function of the magnetic field was determined by measuring the (440) reflection with the  $[1\bar{1}0]$  and the  $[001]$  directions successively parallel to the field. For a given reflection, the field was set at its maximum value, 0.45 T, for 1 sec before opening the counting gate, a counting of 5 sec was collected at the peak position for one direction of the field, then the field was reversed. This sequence was repeated during 15 to 30 min. This fixed time operating mode avoids possible uncorrelated drifts between monitor and detector and limits the statistical errors to only the detector measurements. In order to get a good determination of the peak-to-background ratio wide enough  $2\theta$  scans were made before starting the sequence at each Bragg peak and each energy. Measurements at different positions in the background confirmed a null asymmetry ratio in the background. The peak-to-background ratio being strongly affected by the fluorescence, it allowed us to check the calibration in energy with respect to the Pt  $L_{III}$  edge. For each sequence of measurements, the set of intensities counted by both the monitor and the detector was analyzed by means of a Fourier transform. The beam lifetime, 50 h had a negligible effect. When, for any reason, a significant drift could be ascertained, the result was corrected for, and when fluctuations, larger than the statistical errors, could be detected the error bar was accordingly increased.

## RESULTS

The asymmetry ratios, corrected from the background, have been determined and are reported in Fig. 3. Beyond

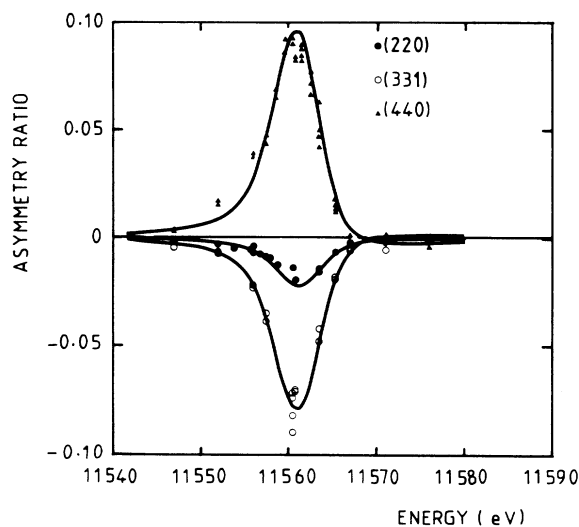


FIG. 3. Energy line shape of the asymmetry ratios for the (220), (331), and (440) reflections. The full lines represent the fits calculated within the assumption of electric dipole  $2p - 5d$  transitions [Eq. (7)].

20 eV below and above the energy of the resonance the values of the asymmetry ratio are negligible. Normal magnetic scattering is too weak to be observed. Closer to the resonance these ratios rapidly increase and reach at the absorption edge values as large as  $-0.012$ ,  $-0.07$ , and  $0.09$  for the (220), (331), and the (440) reflections, respectively. The asymmetrical shape of the curves is qualitatively explained by an interference between the imaginary part of  $a_{res}$  (2) (it behaves like a Lorentzian multiplied by  $x$ ), and  $f''$  (6). The change in sign of the experimental ratio between the (220), (331), and the (440) reflections results from the factor  $\tan(2\theta_B)$  in the Eq. (7), since for the (440) reflection, the Bragg angle is greater than  $45^\circ$ . In Fig. 4 are shown the variations of the asymmetry ratio as a function of the magnetic field. The asymmetry ratios are determined at the maximum of the resonance from the (440) Bragg reflection with the field applied along the  $[110]$  and  $[001]$  directions of the crystal. The anisotropy of the asymmetry ratio between the two directions agrees with the bulk magnetization measurements, but x-rays show a higher initial susceptibility along both directions. This behavior may be due to both methods probing different regions of the sample. The x-ray beam impinges the central zone of the disk, where a smaller density of reverse domains is expected.

We have attempted to fit experimental data using Eq. (7) for the asymmetry ratio. As said above, a single resonance energy is assumed in the calculations. Though the incident beam is not totally polarized in the horizontal plane, the third term in Eq. (2) remains small and is neglected in the calculations. Expression (7) depends on the five parameters  $n_c, n_s, n_{cs}, n_p, n_m$  [see Eq. (6) and associated text], on the polarization  $P_{\parallel}$  and on the width  $\Gamma$  of the resonance. We also have assumed an experimental energy resolution  $\sigma$ . However, the data can be well fitted using previously determined values for some of these parameters and adjusting four of them. The values for  $n_{cs}$  and  $n_s$  are taken from the work by D. H. and L. K. Tem-

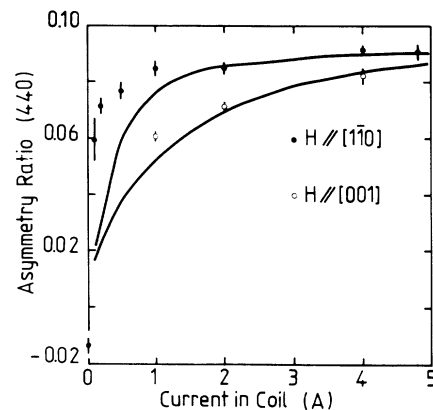


FIG. 4. Variation of the asymmetry ratio as a function of the magnetic field at the (440) Bragg reflection. 1 A corresponds approximately to 0.1 T. Full dots are measured with the field applied along the  $[1\bar{1}0]$  axis of the crystal and open dots with the field along the  $[001]$  axis. Full lines represent the measured magnetization reported in Fig. 1 and multiplied by an appropriate factor.

TABLE I. Values of the parameters used in the fit of the asymmetry ratios as a function of energy and Bragg angle. Only the parameters marked by a (\*) were left free. The others were obtained from a referenced work, or independently measured.

Parameter	Value
Polarization	$P_{  }=0.968$ (measured)
Resonance energy	$E=11\,561.7$ eV (*)
Resonance width	$\Gamma=4$ eV (Ref. 19)
Experimental resolution	$\sigma=1.7$ eV (*)
$f'$ minimum	$n_c=-21r_0$ (*)
$f''$ step	$n_s=6.5r_0$ (Ref. 18)
$f''$ below edge	$n_{cs}=5r_0$ (Ref. 18)
White line	$n_p=4.3r_0$ (Ref. 7)
Magnetic amplitude	$n_m=-0.8r_0$ (*)

pleton on a chloroplatinate:<sup>18</sup> below the edge,  $n_{cs}=5$  electrons and above  $n_{cs}+n_s=11.5$  electrons. The white line amplitude,  $n_p=4.3$  electrons, is obtained from the absorption measurements by Schütz *et al.* on a CoPt alloy.<sup>7</sup> The resonance width  $\Gamma$  is fixed as 4 eV, from the compilation by Bambinek *et al.*<sup>19</sup> The values and status of all parameters are summarized in Table I.

In the present fits the resonance is found at 11 561.7 eV, with an experimental resolution of 1.7 eV. The energy is slightly shifted from the expected value, 11 564 eV, but the difference is not significant since no effort has been made for a precise calibration. Also the resolution is strongly correlated to the value chosen for  $\Gamma$ . The constant  $n_c$  in  $f'$  is found to be  $-21$  electrons, which is consistent with Ref. 18. As the main result, the magnetization-dependent amplitude  $n_m$  has been adjusted

to  $-0.8$  electrons. It is in fairly good agreement with the value ( $-1.1$  electrons), adjusted to fit circular dichroism experiments on CoPt alloy from Schütz *et al.*<sup>7</sup>

## CONCLUSION

Present experiments have shown that observable effects, dependent on the magnetization, can be measured on the coherent scattering amplitude by x-ray resonant scattering in ferromagnetic systems. In CoPt the energy line shape of the asymmetry ratios has been experimentally determined near the  $L_{III}$  absorption edge of Pt. Asymmetry ratios may have rather large values, up to 9% for Bragg angles in the range  $35-55^\circ$ , even though the magnetic moment held by Pt atoms is small. The energy line shape and the variation from one Bragg peak to another are well fitted on the basis of a single electric dipole  $2p-5d$  transitions and a maximum amplitude for magnetic scattering equal to  $-0.8$  electron radius per platinum atom. This agrees with circular dichroism measured by Schütz *et al.*<sup>7</sup> and the order of magnitude is within the theoretical predictions made by Carra, Altarelli, and de Bergevin<sup>10</sup> for the similar alloy MnPt<sub>3</sub>.

## ACKNOWLEDGMENTS

P. Carra and M. Altarelli initiated this work and have greatly contributed to it through encouragement and discussions. We are grateful to Pr. F. Menzinger, who kindly supplied the single crystal. The electromagnet was designed by A. Draperi, and C. Mouget has realized the electronic control system of this experiment. Thanks are given to them.

- <sup>1</sup>D. Gibbs, D. R. Harshman, E. D. Isaacs, D. B. McWhan, D. Mills, and C. Vettier, Phys. Rev. Lett. **61**, 1241 (1988); D. Gibbs, G. Grübel, D. R. Harshman, E. D. Isaacs, D. B. McWhan, D. Mills, and C. Vettier, Phys. Rev. B **43**, 5663 (1991).  
<sup>2</sup>E. D. Isaacs, D. B. McWhan, C. Peters, G. E. Ice, D. P. Siddons, J. B. Hastings, C. Vettier, and O. Vogt, Phys. Rev. Lett. **62**, 1671 (1989).  
<sup>3</sup>J. P. Hannon, G. T. Trammel, M. Blume, and D. Gibbs, Phys. Rev. Lett. **61**, 1245 (1988).  
<sup>4</sup>G. Schütz, W. Wagner, W. Wilhelm, P. Kienle, R. Zeller, R. Frahm, and G. Materlik, Phys. Rev. Lett. **58**, 737 (1987).  
<sup>5</sup>G. Schütz, M. Knülle, R. Wienke, W. Wilhelm, W. Wagner, P. Kienle, and R. Frahm, Z. Phys. B **73**, 67 (1988).  
<sup>6</sup>G. Schütz, R. Wienke, W. Wilhelm, W. Wagner, P. Kienle, R. Zeller, and R. Frahm, Z. Phys. B **75**, 495 (1989).  
<sup>7</sup>G. Schütz, R. Wienke, W. Wilhelm, W. B. Zeper, H. Ebert, and K. Spörl, J. Appl. Phys. **67**, 4456 (1990).  
<sup>8</sup>F. Baudelet, C. Brouder, E. Dartyge, A. Fontaine, J. P. Kappler, and G. Krill, Europhys. Lett. **13**, 751 (1990).  
<sup>9</sup>K. Namikawa, M. Ando, T. Nakajima, and H. Kawata, J.

Phys. Soc. Jpn. **54**, 4099 (1985).

- <sup>10</sup>P. Carra, M. Altarelli, and F. de Bergevin, Phys. Rev. B **40**, 7324 (1989).  
<sup>11</sup>C. Kao, J. B. Hastings, E. D. Johnson, D. P. Siddons, G. C. Smith, and G. A. Prinz, Phys. Rev. Lett. **65**, 373 (1990).  
<sup>12</sup>E. P. Wolfarth, Adv. Phys. **8**, 87 (1959).  
<sup>13</sup>D. Treves, J. T. Jacobs, and E. Sawatzky, J. Appl. Phys. **46**, 2760 (1975).  
<sup>14</sup>N. N. Evtikhiev, N. A. Ekonomov, A. R. Krebs, N. A. Zamyatina, A. S. Komalov, V. G. Pinko, and L. V. Ivaeva, Phys. Status Solidi A **50**, K153 (1978).  
<sup>15</sup>B. Van Laar, J. Phys. (Paris) **25**, 600 (1964).  
<sup>16</sup>F. Menzinger and A. Paoletti, Phys. Rev. **143**, 365 (1966).  
<sup>17</sup>M. Bessière, G. Bessenay, J. Frouin, M. Jouvin, and S. Lefebvre, Nucl. Instrum. Methods A **261**, 591 (1987).  
<sup>18</sup>D. H. Templeton and L. K. Templeton, Acta. Cryst. A **41**, 365 (1985).  
<sup>19</sup>W. Bambinek, B. Crasemann, R. W. Fink, U. H. Freund, H. Mark, C. D. Swift, R. E. Price, and P. V. Rao, Rev. Mod. Phys. **44**, 716 (1972).